Accumulated Aggregation Shifting and Its Application to Robust Defect Detection on SHIBO Surfaces in Real Industry

閆 亞萍†, 項 聖†, 浅野 裕一‡, 金子 俊一†

Yaping YAN†, Sheng XIANG†, Hirokazu ASANO‡, and Shun'ichi KANEKO†

†:北海道大学情報科学研究科
‡:華為技術日本株式会社
yanyaping@hce.ist.hokudai.ac.jp

1. Introduction

The appearance of product is vital to make a good impression on customers. However, during the manufacturing and assembling processes, various defects may be introduced on the surfaces of products, making the automated visual inspection (AVI) highly desirable. This study aims to detect defects on the coated plastic components of industrial products, and especially focus on the background of 'SHIBO' surfaces, which have been widely applied on routers, smart phones, and so on. The non-uniform intensity of faultless region and the low-contrast of defect with no clear edges deter the use of simple thresholding and gradient-based methods. Some other learning based methods makes a large time cost, and it is difficult to collect plenty of good and bad samples [1].

Recently, reliable estimation of visual saliency has been widely used in many computer vision tasks including image segmentation, object recognition. Since the background of SHIBO surface is nearly uniform, defects can be regarded as salient image regions. So we firstly propose two novel features, named the local-global intensity difference and local intensity aggregation, to measure the saliency of pixels. These two features are further used to construct the accumulated aggregation shifting (AAS) model, which can iteratively shift intensity of each pixel according with its defective probability. Our method is unsupervised and training-free. Finally, two fitting models are proposed to classify pixels as defective ones and defect-free ones. Only several samples are needed for parameter optimization.

2. Method

2.1. Salient features

It can be found that real defects usually have intensity difference with the background. We utilize the mode intensity, the intensity value appears most often on the background, as the intensity of background. Then for each pixel, its intensity deviation from the background can be defined

$$r_{ij} = x_{ij} - x_{\text{mode}}, \tag{1}$$

where x_{ij} and x_{mode} denote the intensity of the pixel at (i,

j) and the mode intensity, respectively. Since the background of SHIBO surface is nearly uniform, defect can be regarded as salient regions in surface images. It is reasonable that larger absolute value of intensity deviation means higher saliency and defective degree.

In addition, we find that defective pixels share similar intensities with their neighbors, which can be called the local intensity aggregation. To measure such aggregation, for each pixel, we consider its 5×5 neighborhood, and compare their intensities by

$$a\left(x_{ij}, x_{pq}\right) = \begin{cases} 1, & \left|x_{ij} - x_{pq}\right| \le C_T \left|x_{ij} - x_{\text{mode}}\right|, \\ 0, & \text{otherwise} \end{cases} \tag{2}$$

where C_T is a positive constant to build a direct relation between the threshold and intensity deviation. Here we set as 0.2 from experiments.

Besides, neighbors with different spatial distances to the center pixel have different effects on the local intensity aggregation. We therefore define a distance weight by using a spatially truncated Gaussian kernel. Finally, the local aggregation can be obtained by

$$A_{ij} = \sum_{pq} w_d\left(x_{ij}, x_{pq}\right) \times a\left(x_{ij}, x_{pq}\right). \tag{3}$$

Similarly, higher local intensity aggregation means higher saliency.

2.2. AAS model

Based on the intensity deviation and local aggregation, we propose a novel iterative brightness-shifting model as

$$x[k+1] = x[k] + g \cdot \left(x[k] - x_{\text{mode}}\right), \tag{4}$$

where g is the enhancement factor. With iterations, intensities of all pixels move away from the background intensity, and the moving speed is flexibly decided by g. To locate defective pixels, g is associated with defective probability and defined as the multiplication of normalized local-global intensity difference and local aggregation. Then pixels with higher defective degree will shift faster than the ones with lower defective degree. With iterations, brightness of all defective pixels will be separated with defect-free pixels. It can be deduced from iterative process of

equation (4) that

$$x[k] - x[0] = \left[(1+g)^k - 1 \right] \cdot \left(x[0] - x_{\text{mode}} \right). \quad (5)$$

Therefore AAS output can be regarded as an exponential function of the enhancement coefficient g. Besides, for pixels with low defective probability, their enhancement coefficients are always small enough. By using Taylor-series expansion, we can obtain

$$x[k] - x[0] \approx k \ln(1+g) \left(x[0] - x_{\text{mode}} \right). \quad (6)$$

That is to say, for pixels with low defective probability, AAS outputs can be approximated by a linear function of g. So we utilize a defective model $f_D(k) = a_1 \times b_1^k$, and a defect-free (normal) model $f_N(k) = a_2 \times k + b_2$, to fit the AAS output sequence, with least squares method (LSE). Then the residual sum of squares (RSS), which denotes the discrepancy between AAS outputs and fitting model can be used to judge pixel is defective or not, i.e.,

$$\varepsilon[K] = \sum_{k=1}^{K} \left(x[k] - f_D(k) \right)^2 \bigg/ \sum_{k=1}^{K} \left(x[k] - f_N(k) \right)^2. \quad (7)$$

Classification threshold has a significant influence on the detection performance. Here two-type errors in the hypothesis test are utilized to obtain the optimal value of. There exists a common assumption that residual values of LSE method follow Gaussian distribution with an expectation of zero, so

$$\frac{\varepsilon}{\sigma_D^2 / \sigma_N^2} \sim F(K-1, K-1), \quad (8)$$

The different variances of defect-free and defective pixels lead to different distributions of ε. The probability of two types of errors in the hypothesis test, i.e. P_{FP} (defect-free pixels falsely labeled as defective class) and P_{FN} (defective pixels falsely labeled as defect-free class) can be calculated by

$$P_{FP} = \int_0^{T_\varepsilon} p_f \left(\frac{\varepsilon}{\left(\hat{\sigma}_D^N \right)^2 / \left(\hat{\sigma}_N^N \right)^2} \right) d\varepsilon, \quad (9)$$

$$P_{FN} = 1 - \int_0^{T_\varepsilon} p_f \left(\frac{\varepsilon}{\left(\hat{\sigma}_D^D \right)^2 / \left(\sigma_N^D \right)^2} \right) d\varepsilon, \quad (10)$$

respectively. Finally, the optimal threshold value can be obtained by minimizing the error loss which defined as

$$P_E = c_1 P_{FP} + c_2 P_{FN} \quad (11)$$

3. Experimental results

To verify the performance of the proposed method, we conducted experiments on real-world industrial products' surfaces, and compared with the anisotropic diffusion model with generalized diffusion coefficient function [2] and the phase only transform (PHOT) algorithm [3]. Fig. 1 shows eight representative detection results. From top to bottom are test images, ground truth, inspection results of diffusion model, PHOT, the AAS, and AAS with morphological operator

(AASM), respectively. As can be seen from Fig. 1, the detected defects by all three methods are roughly consistent with the ground truth. However, the PHOT is powerless for scratches. The diffusion model has expansion effect on defects. Comparing to them, our approach is more accurate and stable. The quantitative evaluation results in pixel level are listed in Table 1. As can be seen from Table 1, our approach achieved the best F-measure scores in 6 out of the 8 tests, and exhibits the best performance in terms of Precision, and F-measure scores on the whole database. In conclusion, the proposed method can effectively detect defects with different shapes, size, and contrast.
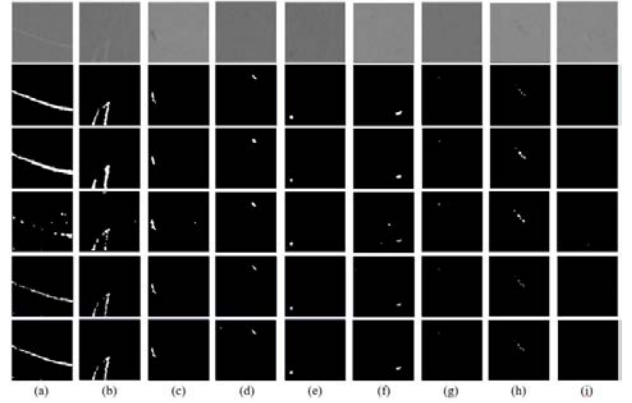

Fig.1. Detection results of various defects.

Table 1: Performance evaluation for defect detection

Sample	Precision				Recall				F-measure			
	Diff.	PHOT	AAS	AASM	Diff.	PHOT	AAS	AASM	Diff.	PHOT	AAS	AASM
(a)	0.7827	0.7093	**0.9557**	0.9638	**0.9606**	0.2492	0.4265	0.6874	**0.8653**	0.3689	0.5726	0.8024
(b)	0.7881	0.7027	**0.9040**	0.8790	**0.9297**	0.7263	0.7119	0.8514	0.8530	0.7143	0.7948	**0.8651**
(c)	0.7235	0.5836	**0.8618**	0.8297	0.6872	**0.9111**	0.7318	0.7597	0.7049	0.7115	0.7915	**0.7927**
(d)	**0.8571**	0.5882	**0.8571**	**0.8571**	0.8571	**0.9892**	0.8571	0.8571	**0.8571**	0.7115	**0.8571**	**0.8571**
(e)	0.9157	0.8017	**0.9924**	0.9755	0.7103	**0.9065**	0.5989	0.7102	0.8000	**0.8509**	0.7487	0.8312
(f)	0.7274	0.7030	**0.9767**	0.9767	**0.8422**	0.4834	0.5854	0.7718	0.7806	0.5729	0.7310	**0.8625**
(g)	0.6423	0.7069	**0.9724**	0.8693	0.8061	**0.8367**	0.7141	0.8164	0.7149	0.7664	0.8235	**0.8429**
(h)	0.3312	0.3312	0.6882	**0.7167**	0.9444	**0.9630**	0.6556	0.7852	0.4904	0.4929	0.6714	**0.7491**
overall	0.7880	0.6693	**0.9355**	0.9076	0.8032	0.6762	0.6150	**0.7577**	0.7882	0.6404	0.7238	**0.8228**

4. Conclusions

In this paper, an accumulated aggregation shifting based salient feature enhancement approach has been proposed for detecting defects on micro 3D textured low-contrast surfaces. It is free from relaying on large amount of labeled data. Experimental results on real industrial images prove the effectiveness of our approach. In the future, the proposed approach will be applied to more kinds of products for quality control.

References

[1] V. A. Sindagi and S. Srivastava, "Domain Adaptation for Automatic OLED Panel Defect Detection Using Adaptive Support Vector Data Description," International Journal of Computer Vision, vol.122, no.2, pp.1-19, 2016.

[2] S. Chao and D. Tsai, "Anisotropic diffusion with generalized diffusion coefficient function for defect detection in low-contrast surface images," Pattern Recognition, vol. 43, 2010, pp. 1917-1931

[3] D. Aiger and H. Talbot, "The phase only transform for unsupervised surface defect detection," in proc. of IEEE Conference on Computer Vision and Pattern Recognition (CVPR), 2010, pp. 295-302.